고분자막과 다층구조를 이용한 가변렌즈기반 광학 줌 시스템

Dan Liang[†], Dong Tai Liang, and Xuan Yin Wang*

Faculty of Mechanical Engineering and Mechanics, Ningbo University
*The State Key Laboratory of Fluid Power and Mechatronic Systems, Zhejiang University
(2018년 5월 30일 접수, 2018년 7월 20일 수정, 2018년 7월 29일 채택)

An Optical Zoom System Based on Tunable Lens with Polymer Membrane and Multilayered Structure

Dan Liang[†], Dong Tai Liang, and Xuan Yin Wang*

*Faculty of Mechanical Engineering and Mechanics, Ningbo University, 818 Fenghua Rd., Ningbo City,
Zhejiang Province, 315211, P. R. China*
**The State Key Laboratory of Fluid Power and Mechatronic Systems, Zhejiang University,
38 Zheda Road, Hangzhou, 310027, P. R. China*
(Received May 30, 2018; Revised July 20, 2018; Accepted July 29, 2018)

Abstract: We have developed an optical zoom system based on tunable lens with polymer membrane and multilayered structure. The presented system employed two tunable lenses and two doublet lenses as the main refractive units. Each tunable lens had a delicately designed, solid-liquid mixed structure with multiple internal slim holes, which helped to improve the lens optical properties and stability against gravity. The optical structure and regulation principle of the zoom system is presented, as well as the detailed fabrication process of the tunable lens. Under different displacement loads, the lens deformation properties, and the adjustment ability and imaging characteristics of the zoom system were measured and analyzed. Besides, the spot diagram, field curvature and distortion of the system were simulated using the Zemax software. The magnification of the designed system could be regulated from 0.2X to 4.3X flexibly depending on the focal variation of each tunable lens.

Keywords: zoom system, polymer membrane, tunable lens, integrated structure.

Introduction

Zoom system is often found in many optical applications such as cell phones, microscopes, telescopes, pico projectors and digital cameras.[1-3] With development of the optics technology, the requirements for integration, flexibility and adjustment ability of the zoom system become higher and higher. Therefore, it is of great necessity to develop the zoom system with compact structure, stable optical property and large magnification ratio.

The conventional optical zoom system generally consists of multiple solid lens groups, electrical motors and transmission mechanisms, which usually has limited magnification ratio,

bulky package and complicated driving module. Recent years, the tunable lenses with adjustable focus have attracts much attention,[4-6] showing the potential to be used for various flexible zoom systems. According to regulating principle, the focus of tunable lens can be adjusted by changing the lens refractive index or the lens surface shape. The liquid crystal (LC) lens is a typical kind of tunable lens, which controls the refractive index through altering the molecular distribution structure of the LC material.[7] Utilizing two LC lenses as the main adjustable unit, an electrically tunable-focusing zoom system was presented, which realized a zoom ratio of 7.9:1.[8] A optical imaging system was demonstrated which used one LC lens to maintain the imaging position and two other LC lenses in charge of zoom function.[9] Due to the existed inhomogeneity of the LC material, the LC lens system was usually faced with the problems of energy loss and optical distortions.

The liquid tunable lens adjusted the focus by changing the

shape of lens refractive surfaces, such as electro-wetting lens, the fluidic tunable lens, and dielectric elastomer lens.[10-12] Various optical imaging systems were developed and analyzed using the liquid tunable lens. For example, a two-liquid-lens zoom system without moving elements was reported which had a zoom factor of 1.8 and a compact structure of 10 mm.[13] An optofluidic zoom system was presented which utilizes liquid optical path switchers to reduce the structure and increase the zoom range.[14] A three-element zoom system for laser beam expanders based on liquid tunable lens was presented, as well as the design principle and paraxial properties of the system.[15] The electrowetting based liquid tunable lens has compact structure and large zoom range, but this kind of tunable lens and imaging system usually had a small aperture and requires a relatively high voltage. The pressure driven liquid lens mainly consists of elastic membrane, optical liquid and holder, and adjust the focus through changing the liquid pressure to alter the lens surface deformation.[16,17] This kind of tunable lens had good integration, strong adjustability and flexible aperture, showing broad application potentials. As the liquid material is usually susceptible to the external vibration and gravity effect, the stability and optical properties of the pressure driven tunable lens and imaging system remains to be improved.

In this paper, we have developed an optical zoom system based on tunable lens with polymer membrane and multi-layered structure. Compared with the previous zoom system based on liquid tunable lens, we used a solid-liquid mixed structure with multiple slim holes to design the porous tunable lens, in order to improve the stability and optical quality of the zoom system. Each tunable lens was made of solid-liquid mixed material with multiple optical layers, which would not only reduce the proportion of the liquid to improve the lens stability, but also offer more optical freedoms for the practical applications. Besides, multiple slim holes were drilled in the front aperture, inner lens and holder of the tunable lens, which can increase the fluidic damping resistance to improve the lens adaptability to gravity and enhance the stability of the optical axis. In the following section, the optical structure and regulation principle of the zoom system are presented, as well as the detailed fabrication process of the tunable lens. Under different displacement loads, the lens deformation property, adjustment ability and imaging characteristics of the zoom system were measured and analyzed. Furthermore, the spot diagram, field curvature and distortion of the presented system are also discussed.

Design and Fabrication Process

Optical Structure of the Zoom System. The traditional zoom system controls the movement of each lens group to maintain a fixed image location while adjusting the optical zoom power of the system, which usually needs complicated transmission and driving mechanisms. The tunable lens technology offers another way to adjust the zoom power: by changing the diopter of each lens rather than changing the lens position. Variable zoom power could be achieved through synchronizing two or more fluidic tunable lenses. In this paper, our primary focus is to design a prototype zoom system mainly consisting of several flexible tunable lenses and solid lenses, which has large magnification ratio and good stability simultaneously.

As shown in Figure 1, the presented zoom system consists of an object collimated doublet lens, two tunable lenses, an fixed focusing doublet lens, and a CCD sensor. Each tunable lens has an elastic surface which can get compressed flexibly by the external pressure. By squeezing the surface of the tunable lens with a rigid compression ring, the lens surface curvature can be adjusted continuously, leading to the variation of the focal length. The two tunable lenses make up the zoom module of the system, while the fixed focusing lens and CCD sensor constitute the camera system. The proposed tunable lens has a solid-liquid mixed structure with series of multiple slim holes, which consists of a holder, an elastic polymer membrane, a porous aperture, a multi-hole inner lens, a rigid back lens and optical liquid (Figure 2). The advantages of the designed structure for the tunable lens are as follows. Firstly, utilizing the solid-liquid structure helps to reduce the proportion of the liquid material while maintaining the adjustment ability of the lens focus. Secondly, multiple interconnected slim holes are drilled in the porous aperture, holder and inner lens, which would help to improve the lens resistance to gravity through increasing the fluidic damping forces. Thirdly, the designed tunable lens has multiple optical layers, offering more design and optimization freedoms for the practical applications than the monolayer lens.

The zooming module of the system mainly consists of two tunable lenses. According to the paraxial optics theory,[18] the optical power of the zooming module can be computed by

$$D = D_1 + D_2 - SD_1D_2 = \frac{1}{f_1} + \frac{1}{f_2} - \frac{S}{f_1 f_2} \qquad (1)$$

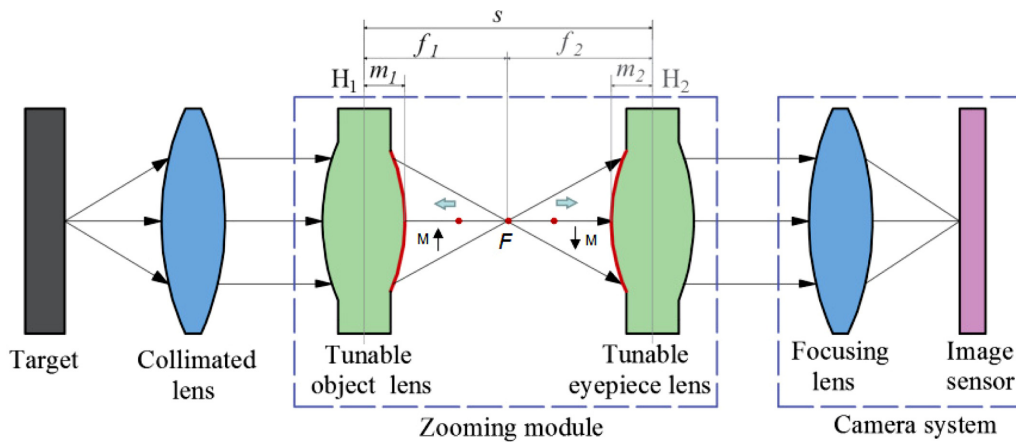where D is the total optical power of the two tunable lenses, D_1

Figure 1. Schematic diagram of the optical zoom system based on multilayered tunable lens, M means magnification ratio. When the common focus F of the tunable lenses moves left, M would increases. When the common focus moves right, M would get smaller.
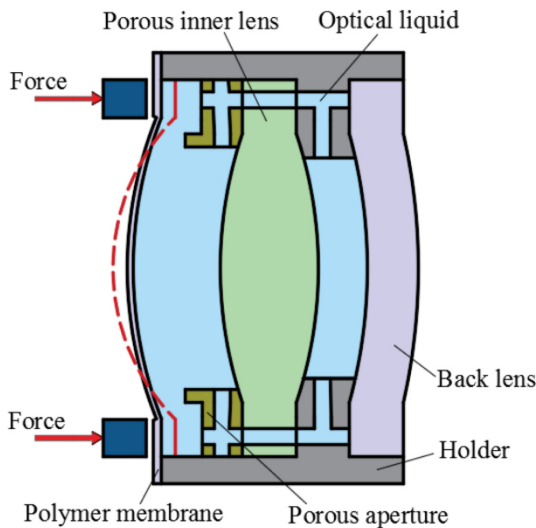

Figure 2. The structure of the designed tunable lens with multiple slim holes. The red line shows the surface deformation of the elastic polymer membrane when compressed by the external pressure.

and f_1 are the optical power and effective focal length of tunable lens 1 separately, D_2 and f_2 are the optical power and effective focal length of the tunable lens 2 respectively, and S is the optical distance between the image principal planes of the two tunable lenses.

In order to focus the object light onto the CCD sensor correctly, the CCD sensor need to be placed on the focal region of the back focusing lens, and the total optical power of the two tunable lenses should be near the value of 0. Therefore, the distance between the two tunable lenses need satisfy $S = f_1 + f_2$, to keep the two lenses afocal. Define the optical distance between the image principle plane and back surface of the tunable lens

1 as m_1, the distance between the image principle plane and front surface of the tunable lens 2 as m_2, the back focal length of tunable lens 1 as l_1, the front focal length of the tunable lens 2 as l_2, and the distance between the back surface of tunable lens 1 and front surface of lens 2 as l, then

$$S = l + m_1 + m_2 = l_1 + m_1 + l_2 + m_2 = f_1 + f_2 \tag{2}$$

Therefore, the equation $l = l_1 + l_2$ equals $S = f_1 + f_2$. The focal length of the two tunable lenses can get adjusted by the external compression ring independently. The compression ring can be connected with the universal camera driving devices such as coil motor and ultrasonic motor. Through controlling the displacement of the compression ring to extrude the tunable lens, we can alter the lens surface to adjust the focal length flexibly. The magnification of the system can be computed by $M = f_2/f_1$, and the imaging position is located at the focal region of the back focusing lens.

Fabrication Process. The key optical units of the designed zoom system mainly consists of the two tunable lenses, the rigid collimated lens and the back focusing lens. As described above, the tunable lens mainly consists of an elastic polymer membrane, optical liquid, a porous aperture, a porous inner lens and a back lens. The collimated lens and focusing lens used in this paper are commercial doublet lenses. The elastic membrane of the tunable lens is made from PDMS (polydimethylsiloxane) polymer material, which has good elasticity, transparency and chemical stability.[19,20] The back lens in the tunable lens is a rigid commercial PMMA lens, while the porous inner lens is a commercial glass lens with 8 slim holes drilled in the lens fringing area. The porous aperture

and holder are made from the HDPE (high-density polyethylene) material,[21,22] which has high chemical stability, rigidity and mechanical strength. The holder was used to immobilize the whole structure of the tunable lens, and fabricated by a CNC (computer numerical control) lathe using the HDPE material. Eight slim holes are drilled in the middle convex platform of the holder. The optical liquid used in this paper is a kind of commercial synthetic optical liquid from the Cargille Laboratories. The refractive index of the optical liquid was 1.34, and the Abb number was 62.

The elastic membrane was fabricated by the centrifugal spin coating method. The thickness of the elastic membrane was controlled by the rotation speed of the centrifugal machine (TDZ4-WS, HEREXI). Generally speaking, the higher the rotating speed, the thicker the fabricated membrane. The membrane needed enough elasticity to ensure that the tunable lens can get compressed easily under the tiny displacement load. The detailed fabrication process of the tunable lens are as follows. Firstly, the PDMS prepolymer and curing agent are mixed at a mass proportion of 15:1, and get debubbling processed using a vacuum pump. Secondly, the PDMS mixture is dropped onto the silicon base of the centrifuge machine, and get spin-coating processed under the rotation speed of 1200 rpm/min for 30 min. Thirdly, the silicon base coated with PDMS mixture is put into a thermostat under 80 degrees centigrade for 50 min. After the heating process, the PDMS mixture would get fully solidified. Then, the PDMS membrane is peeled off from the silicon base, and cut into thin circular plate with a diameter of 16 mm. In order to make sure that the elastic deformation mainly occurs in the middle photic zone of the membrane, the thickness of the middle area need to be thinner than the peripheral area. Therefore, we fabricate another annular membrane using the same procedure, and bond it onto the circular membrane through the ultraviolet curing process. Finally, we can get the designed membrane with different thickness in the peripheral and middle areas. During the demoulding process, alcohol is dropped onto the interface between the membrane and the silicon base to facilitate the desquamation of the membrane. The roughness of the membrane is also measured using an optical interferometer (NT1100, Veeco), and the root mean square value of the surface roughness is about 3.12 nm. The peripheral thickness of the membrane is 1.2 mm, while the middle area is a little thinner (about 0.6 mm).

Figure 3 shows the assembling process of the presented porous tunable lens. Firstly, the porous inner lens and back lens are fixed into the two grooves in the holder. The slim holes of the inner lens need to be connected tightly with the holes in the holder, in order to ensure that the optical liquid can flow through the different holes fluently. Secondly, the polymer membrane is bonded onto the left surface of the holder using the optical adhesive (TZ312). An empty chamber is then constructed by the elastic membrane, holder and porous inner lens. Thirdly, injecting the optical liquid into the chamber gradually through the slim hole in the flank surface of the holder. A glass lens with specific curvature radius is placed against the polymer membrane in order to maintain the lens initial shape. After the chamber is full of optical liquid, the injection holes in the holder are sealed by the optical glue rigorously. Finally, we need put the assembling lens in a thermostatic chamber under room temperature for 1 h to get standing treatment.

The aperture diameter of the tunable lens is 10 mm, which can be optimized according to the practical applications. Some researches show that,[23,24] when the liquid lens is placed ver-
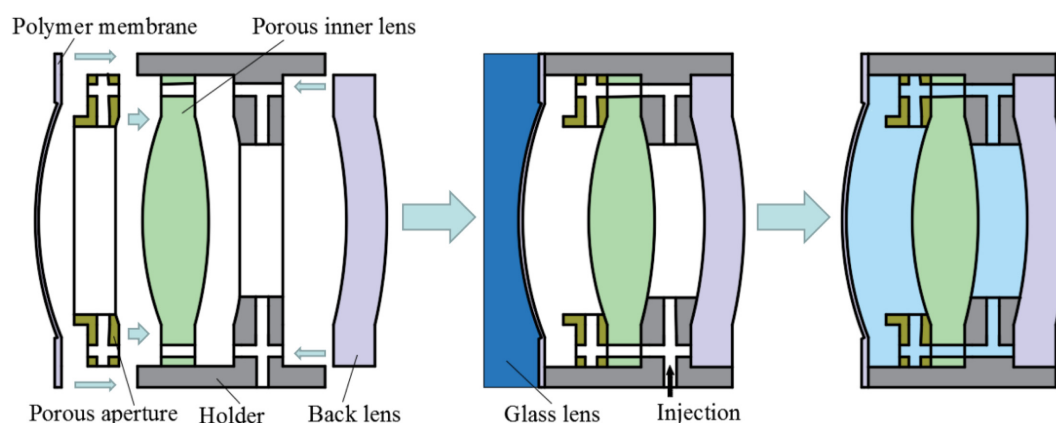

Figure 3. Assembling process of the presented tunable lens.

tically, the lens optical axis would be impacted by the gravity effect apparently. As for the electrowetting lens, the intermolecular tension of the liquid could almost totally counteract the effect of the gravity. But the liquid lens was always faced with the problem of gravity effect and axis instability. In this paper, we used an elaborate structure with solid-liquid mixed multilayered combination to reduce the gravity effect and improve the lens optical properties. The initial parameters of the tunable lens were designed mainly according to the Gullstrand 1 model of human eye,[18] and also got scaled up and optimized through Zemax to facilitate the fabrication process. The theoretical initial diopter of the tunable lens was about 11.4 D. The presented prototype system is used to show the basic principle and fabrication method for the porous tunable lens based optical system. The lens optical structures remained adjusted according to the practical applications. Synthesizing the fabrication process and material properties, the key parameters of the prototype lens are as follows (Table 1). Figure 4 shows the picture of the fabricated elastic membrane and tunable lens. This paper mainly utilizes the PDMS material to fabricate the elastic membrane, the application and comparison of other polymers would be considered in future to further improve the lens adjusting capability and optical properties.

Table 1. Optical Parameters of the Solid-liquid Mixed Tunable Lens under the Initial State

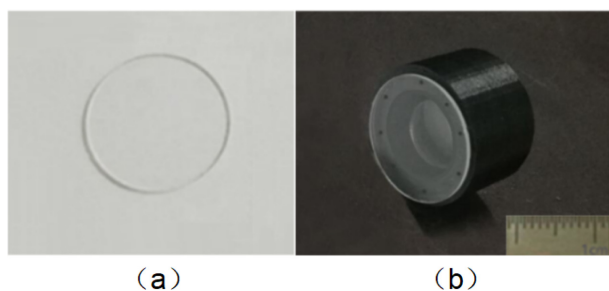| Refr. surface		Curv. radius (mm)	Spacing (mm)	Refr. index
PDMS membrane		92	2.8	1.34
Porous inner lens	Front	86	2.1	1.50
	Rear	-86	2	1.34
Back lens	Front	-90	2.1	1.49
	Rear	-85	-	1

Figure 4. (a) Picture of the fabricated elastic membrane; (b) picture of the fabricated tunable lens.

Experiments and Analyses

Regulation Process of the Tunable Lens. The focal length of the tunable lens under different displacement loads was measured using an optical device based on the traditional collimator method, which obtained the focal length by computing the lens magnifying power. The device mainly consisted of a collimator tube, reading microscope, guide rail and lens compression module, as is shown is Figure 5. The compression module was mainly composed of a compression ring and a micro voice coil motor (VM15002, JinGon). Through controlling the displacement of the compression ring, we could alter the surface shape of the polymer membrane to adjust the lens focus. We used the mean value of 6 multiple measurements as the final result to ensure the accuracy and reliability.

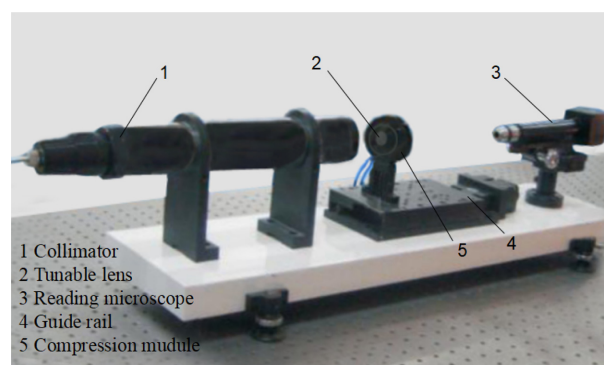Figure 6 shows the relationship among the displacement

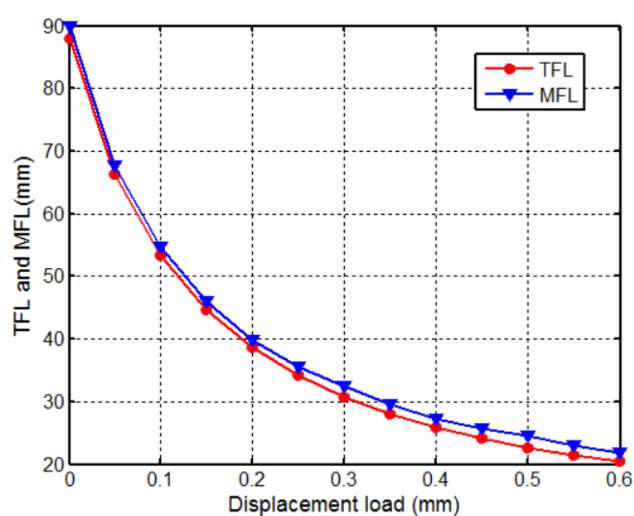**Figure 5.** Optical device used to measure the lens focal length.

Figure 6. Relationship among the displacement load, the TFL and the MFL of the tunable lens.

load, the theoretical effective focal length (TFL) and the measured effective focal length (MFL) of the tunable lens. The TFL was computed according to the axial optics analyses method, and the curvature radius of the lens elastic membrane is obtained by spherical fitting, similar to the method depicted in reference 24. With the increase of the imposed load, the lens elastic membrane protrudes outwards gradually, making the lens MFL become smaller and smaller. Initially, the displacement load was set to be 0 mm, and the corresponding MFL was 87.2 mm. When the displacement load reaches 0.6 mm, the lens MFL gets 20.4 mm, with a diopter of 6.2 D. A 4.27 times alteration of the MFL is achieved by imposing a tiny displacement load of 0.6 mm. The variation of the lens focus was related to the diameter of the compression ring, thickness of the membrane, the optical materials and intervals among each optical layers. Under different displacement loads, the average response time was about 150 to 180 ms. Choosing different structural parameters according to the requirements of practical applications, almost any adjustment range could be achieved theoretically.

Generally speaking, the gravity showed the greatest effect on the liquid tunable lens when placed vertically, especially the lens lower part, which would affect the rotational symmetry of the lens surface appearance. In order to verify the stability of the designed solid-liquid mixed tunable lens to the gravity effect, we placed the lens vertically and divide the lens membrane surface into two parts including the upper half and lower half area separately to measure the deformation process. Figure 7
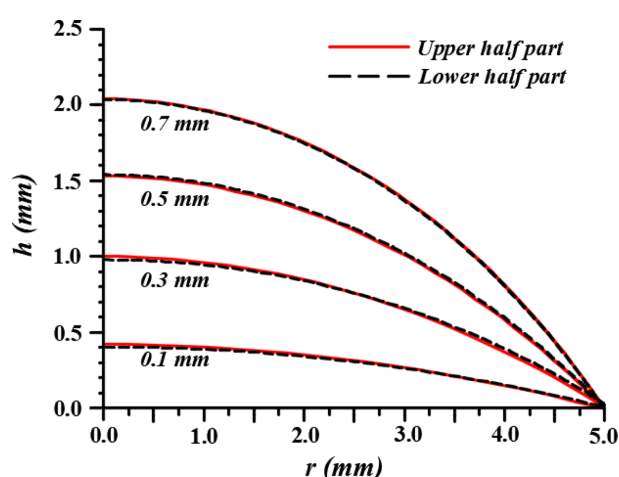

Figure 7. Measurement results of the lens elastic surface in the case of vertical placement. The surface is divided into the upper half and the lower half areas. The solid lines are the measurement results of the upper half area, and the dashed lines are the measurement results of the lower half area.

shows the measurement results of the lens elastic surface in the case of vertical placement. The largest difference between the upper half and lower half curves was less than 0.04%. The difference between the upper and lower halves was rather small, which means that the designed solid-liquid mixed tunable lens could resist the gravity influence effectively and maintain a relatively good rotational symmetry. The existed asymmetry would increase the lens coma and distortion, and impact the imaging quality. Optimizing the fabrication procedure and reducing the proportion of the liquid would help to further maintain the lens symmetry. Under different displacement loads, the curvature radius of the lens was changed rapidly and flexibly.

Zoom System Verification. In order to analyze the zooming ability and imaging properties of the presented system, we designed an experimental system according to the structure depicted in Figure 1. The elastic membrane of the tunable lens was extruded by a rigid compression ring connected to the micrometer stage. Based on our design, the maximum displacement load was set to be 0.6 mm to measure the lens regulating ability under small displacement load. Passing through the two tunable lenses and the back focusing lens, the image of an illuminated letter chart was then projected onto the CCD sensor. The focal distance of the collimated lens and back focusing lens is 28 mm. The clear aperture of the system was about 8 mm. The presented system was a visible imaging system, and the working wavelength was from 390-780 μm. During the experiment, the distance between the two tunable lenses was kept to be 100 mm. Each lens focal distance was adjusted by changing the displacement load through controlling the output of the micrometer stage. The theoretical zoom magnification of the system could be computed by the equation $M = f_2/f_1$. Meanwhile, the experimental magnification could be obtained by the analysis of the image height under each displacement load relative to the image height captured at 1:1 magnification.

Figure 8 shows the relationship among the focal distance of tunable lens 1, the theoretical zoom magnification and experimental magnification. Through controlling the focal distance of each tunable lens, the magnification of the presented system could be adjusted from 0.2X to 4.3X flexibly and reversibly. The ratio of the maximum magnification to the minimum magnification reached 21.5. The maximum error between the theoretical and experimental zoom magnification was about 3.2%. The presented zoom system based on the solid-liquid mixed tunable lens was mainly used to verify the feasibility and optical properties of the designed structure, future work would fur-
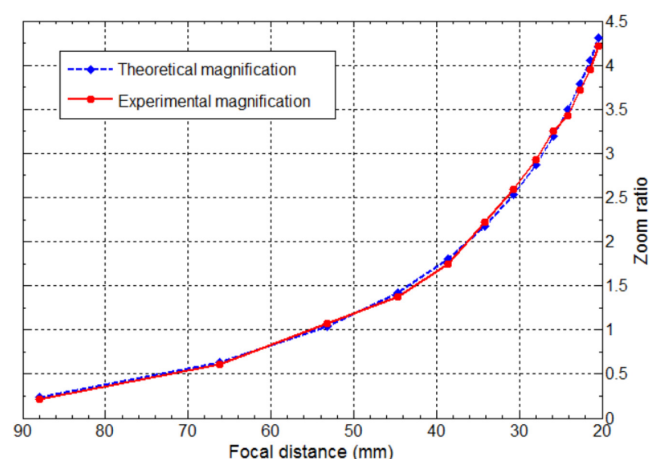
Figure 8. Relationship among the focal distance of tunable lens 1, the theoretical zoom magnification and experimental magnification.
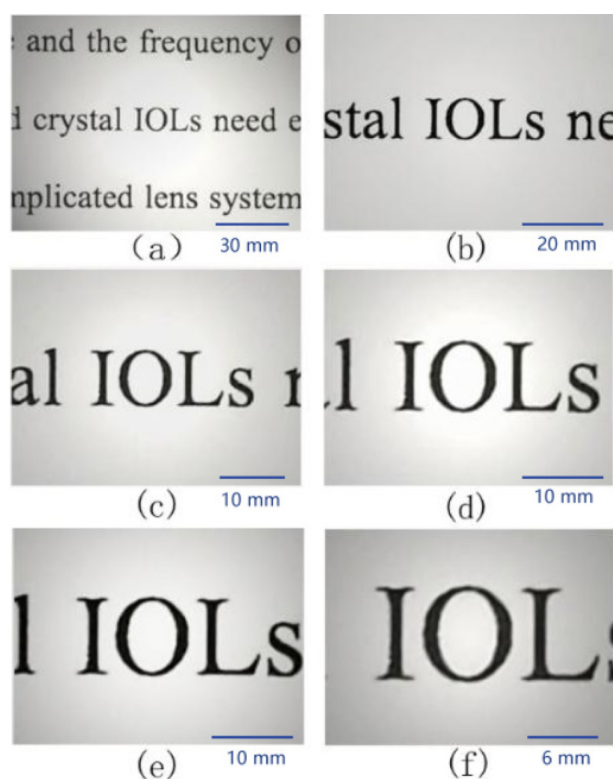

Figure 9. Image performance of the zooming system. From (a) to (d), the magnification ratio is 1.1*X*, 1.8*X*, 2.5*X*, 3.2*X*, 3.5*X* and 4.3*X*, respectively.

ther analyzing the deformation process and optical properties by the finite element methods.

The images captured under different zoom magnifications are shown in Figure 9. From Figure 9(a) to Figure 9(f), the MFL of the front tunable lens is 54.2, 39.6, 32.1, 25.7, 24.5 and 21.2 mm separately. Qualitatively, the designed system
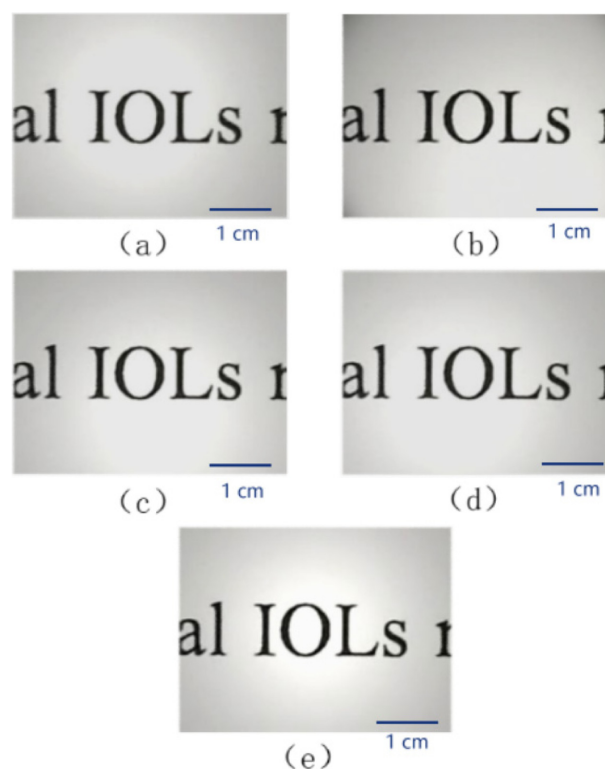

Figure 10. Images captured at different angles under the magnification of 2.5*X*. From picture (a) to (d), the rotating angles are 0 deg, 45 deg, 90 deg, 135 deg and 180 deg, respectively.

could capture relatively clear images under different displacement loads. There exists halo and distortion, which would reduce the luminous flux of the system and impact the imaging quality. The image quality captured during the middle stage of the deformation process was better than the initial and end deformation stage. Choosing the more symmetrical optical structure would improve the imaging quality. When the displacement was relatively large, the image quality was not only impacted by the lens structure, but also impacted by the inherent aberration caused by the highly curved surface. Generally speaking, less curvature led to smaller aberration. As for a highly curved surface, negative conical constants would help to reduce the spherical aberration. At least two ways could be used to optimize the optical quality of the system when the deformation was relatively large, and both ways are relative to the optical freedom offered by the lens components. One way was to utilize the material with higher refractive index, the other was to use the aspheric surface such as conic constant to correct the aberration.

To verify the stability and resistance to the gravity, we placed the zoom system under different rotation angles to con-

duct the imaging experiment. The tunable lens and the whole zoom system were initially put horizontally, and gradually adjusted to 45, 90, 135 and 180 degrees. Figure 10 shows the images captured under different rotation angles. All the images had almost the same optical pattern and quality, showing that the gravity has little effect on the lens deformation and imaging process. By utilizing the solid-liquid material with multilayered structure and increasing the fluidic damping force through the multiple slim holes drilled in the key components of the tunable lens, the lens stability has got improved apparently.

Furthermore, the spot diagram, distortion and field curvature of the presented zoom system were also simulated using the Zemax software, in order to analyze the optical properties numerically. The optical parameters were the same as the structure depicted in section 2. The front and rear surface of the tunable lens are set to be a standard surface with parabolic conic coefficient. The spot diagram referred to the root-mean-square (RMS) spot diagram, which showed the approximate light spot distribution after passing through the optical system. In this section, the spot diagrams under 0 and 10 field of view (FOV) are simulated. Figure 11 shows the RMS simulation
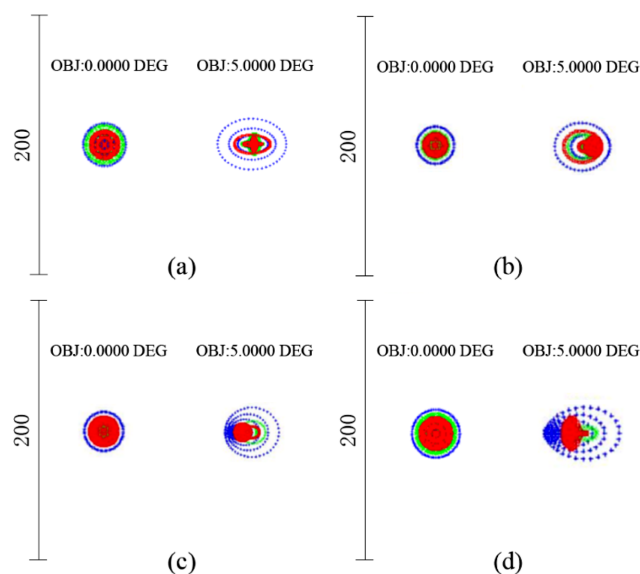

Figure 11. RMS spot diagram of the presented optical system under different magnification ratio. From (a) to (d); the magnification is 0.2X, 1.8X, 3.2X and 4.3X, respectively.

results of the presented zoom system. When the magnification ratios were 0.2X, 1.8X, 3.2X and 4.3X, the RMS radii under 0 field angles were 10.15, 7.26, 8.12, and 12.67 μm, and the
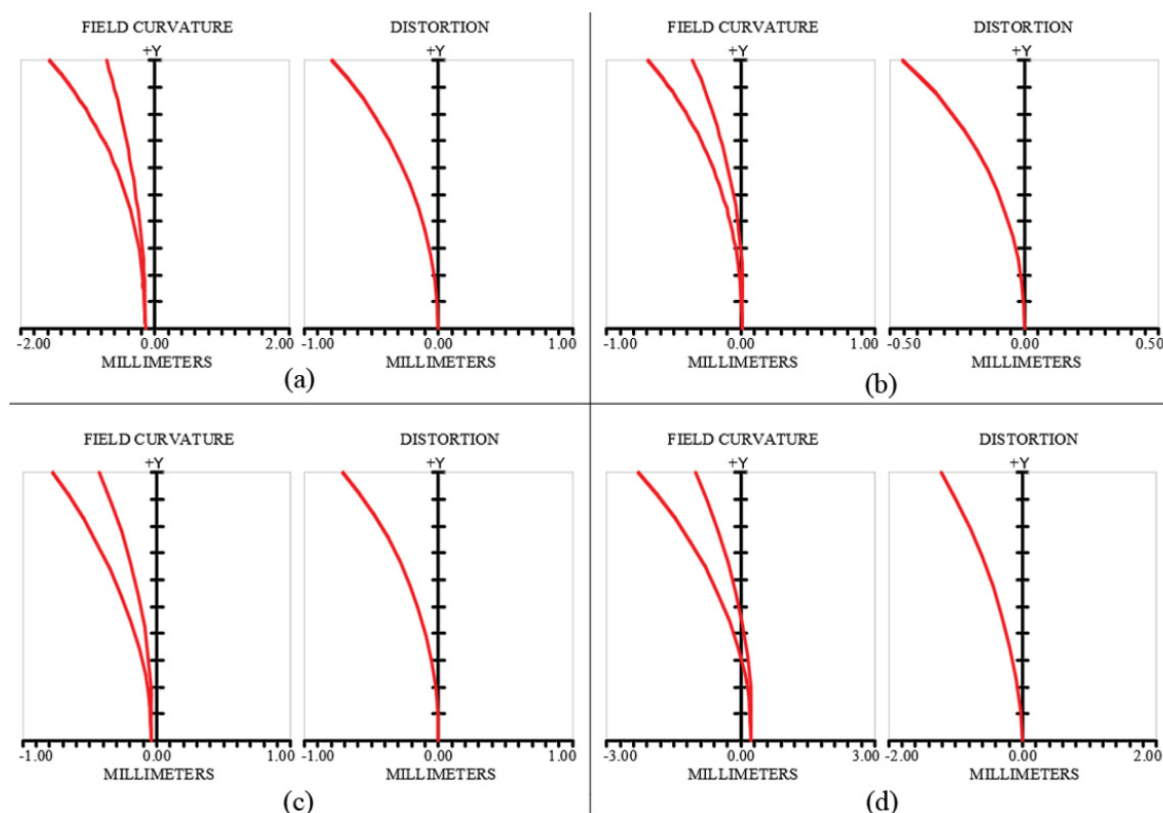

Figure 12. Field curvature/distortion results of the presented system. From (a) to (d); the magnification is 0.2X, 1.8X, 3.2X and 4.3X, respectively.

RMS radii of 10 field views were 19.25, 14.36, 16.12, and 32.28 μm, respectively. Obviously, the RMS simulation results were better in the middle zooming stage than the initial and end stage. Under the 0 field angle, all the raddi of the spot diagram were less than 12.7 μm, and the RMS radius gets larger with the increase of the FOV.

The field curvature plot describes the distance from the currently defined focal image plane to the paraxial focal plane as a function of the field coordinate. Distortion is an index representing the height (length) differences between the real target and captured image. Figure 12 shows the field curvature/distortion results of the designed system. The field of view was set to be 0 and 10 degrees, and the wavelength was 560 nm. The field curvature and distortion under the magnification of 0.2X and 4.3X was larger than the other zooming stage apparently. Under the magnification of 1.8X, the absolute value of the field curvature is 0.76 mm, and the absolute value of the distortion was about 0.5%. The distortion of all cases was less than 1.8%, and the largest astigmatism appears at the edge of the image when the magnification ratio was 4.3X. The presented system showed relatively good optical performance and large magnification ratio, but still needs improvement and optimization. There was some astigmatism, field curvature and distortions, especially in the large field view. Based on the optical analyses theory, the astigmatism, field curvature, and distortion were mainly related to the field of view and aperture. Through optimizing the optical parameters of the two tunable lenses, using the doublet and symmetric optical structure based on the achromatic principle, and designing specific optical filter and auxiliary module, we can further reduce the aberration and improve the imaging quality of the presented zoom system.

Conclusions

In this paper, we have presented a prototype zoom system based on the tunable lens with polymer membrane. Compared with the previous zoom system based on liquid tunable lens, we used a solid-liquid mixed structure with multiple slim holes to design a porous tunable lens, which helped to improve the stability and optical quality of the system. As the key part of the zoom system, the structure, fabrication process, and deformation properties of the porous tunable lens were elaborated. The focal length of the tunable lens ranged from 87.2 to 20.4 mm, and the variation of the diopter reaches 37.6 D. A change in magnification from 0.2X to 4.3X is demonstrated within a

tiny 0.6 mm variation of the displacement load. Images captured under different magnification ratios showed relatively good optical quality. When placed under different rotation angles, the designed system had almost identical deformation mode and imaging pattern, which could significantly resist the gravity effect. Under the 0 field angle, all the raddi of the spot diagram are less than 12.7 μm, and the distortion of all cases is less than 2%. Through optimizing the fabrication process and lens optical structure, utilizing more sophisticated driving system, we could further improve the stability and zooming continuity of the system. The presented system showed the potential to be used in various optical systems such as digital cameras, microscope and telescopes.

References

1. H. Zhao, X. W. Fan, G. Y. Zou, Z. H. Pang, W. Wang, G. R. Ren, Y. F. Du, and Y. Su, *Appl. Optics*, **52**, 1192 (2013).
2. H. Zhou, Y. Liu, Q. Sun, C. Li, X. L. Zhang, and J. B. Huang, *Opt. Eng.*, **52**, 3002 (2013).
3. G. Kim, J. Lee, and H. Noh, *Polym. Korea*, **42**, 427 (2018).
4. W. Li, D. Bryant, and P. J. Bos, *Liq. Cryst. Rev.*, **2**, 130 (2014).
5. X. Y. Wang, D. Liang, F. Tang, and J. W. Du, *Polym. Korea*, **40**, 209 (2016).
6. D. Kopp and H. Zappe, *IEEE Photonic. Tech. L.*, **28**, 597 (2016).
7. H. C. Li and Y. H. Lin, *Appl. Phys. Lett.*, **98**, 063505 (2011).
8. Y. H. Lin, M. S. Chen, and H. C. Lin, *Opt. Express*, **19**, 4714 (2011).
9. M. S. Chen, P. J. Chen, M. Chen, and Y. H. Lin, *Opt. Express*, **22**, 11427 (2014).
10. X. D. Hu, S. G. Zhang, Y. Liu, C. Qu, L. J. Lu, X. Y. Ma, X. P. Zhang, and Y. Q. Deng, *Appl. Phys. Lett.*, **99**, 159 (2011).
11. J. K. Lee, K. W. Park, G. B. Lim, H. R. Kim, and S. H. Kong, *J. Opt. Soc. Korea*, **16**, 22 (2012).
12. S. I. Son, D. Pugal, T. Hwang, H. R. Choi, J. C. Koo, Y. K. Lee, K. K. Kim, and J. D. D. Nam, *Appl. Optics*, **51**, 2987 (2012).
13. D. Li, W. Zhang, and X. Guo, *J. Opt. Soc. Korea*, **17**, 447 (2013).
14. L. Li, R. Y. Yuan, L. Luo, and Q. H. Wang, *IEEE Photonic. Tech. L.*, **99**, 1 (2018).
15. H. T. Cheng, H. Liu, and H. Y. Li, *Opt. Express*, **23**, 12258 (2015).
16. Y. Iimura, H. Onoe, T. Teshima, Y. J. Heo, S. Yoshida, Y.

Morimoto, and S. Takeuchi, *J. Micromech. Microeng.*, **25**, (2015).

17. N. Savidis, G. Peyman, N. Peyghambarian, and J. Schwiegerling, *Appl. Optics*, **52**, 2858 (2013).

18. D. Yu and H. Tan, *Engineering Optics*, 3rd ed., China Machine, Beijing, 2007.

19. S. W. Bak, H. J. Kang, and D. W. Kang, *Polym. Korea*, **38**, 138 (2014).

20. S. H. Ra, H. D. Lee, and Y. H. Kim, *Polym. Korea*, **39,** 579 (2015).

21. E. D. Bliznakov, C. C. White, and M. T. Shaw, *J. Appl. Polym. Sci.*, **77,** 3220 (2015).

22. B. S. Shin, S. T. Jung, J. P. Jeun, H. B. Kim, S. H. Oh, and P. H. Kang, *Polym. Korea*, **36**, 549 (2012).

23. W. Zhang, P. F. Liu, X. N. Wei, S. L. Zhang, and B. Yang, *Proc. SPIE*, 7849 (2010).

24. J. W. Du, X. Y. Wang, S. Q. Zhu, and D. Liang, *Optik*, **130**, 1244 (2017).